TABLE OF CONTENTS

SPECIAL SECTION ON THE SEVENTH BRAZILIAN SYMPOSIUM ON BIOINFORMATICS

REGULAR PAPERS

(Contents continued on inside back cover)

MANUSCRIPT SUBMISSIONS / STATUS INQUIRIES: For information on submitting a manuscript or on a paper awaiting publication, please contact: Transactions Administrator *IEEE/ACM TCBB*, IEEE Computer Society, 10662 Los Vaqueros Circle, Los Alamitos, CA 90720 USA; EMAIL: tcbb@computer.org, PHONE: +1 714.821.8380; FAX: +1 714.821.4010

IEEE/ACM TRANSACTIONS ON COMPUTATIONAL BIOLOGY AND BIOINFORMATICS Vol. 10, No. 4, July-August 2013

VOLUME 10 NUMBER 4 ITCBCY (ISSN 1545-5963)

CELEBRATING 10 YEARS

IEEE/ACM TRANSACTIONS ON

COMPUTATIONAL BIOLOGY AND BIOINFORMATICS

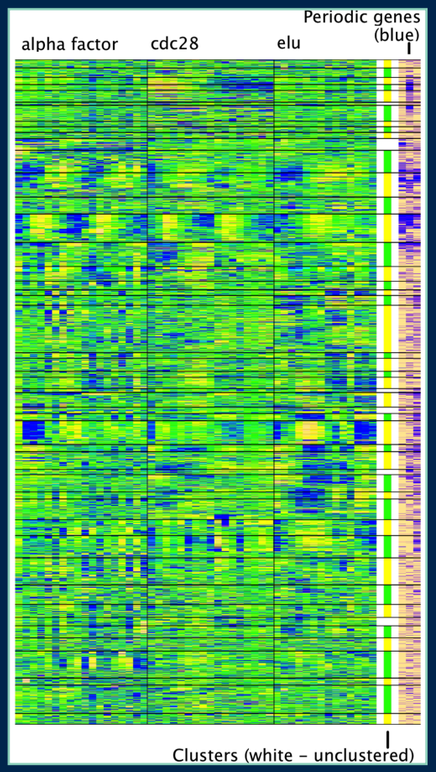

JULY-AUGUST 2013

Indexed in MEDLINE®/PubMed® and indexed in ISI

MEDLINE U.S. National Library of Medicine PubMed

IEEE acm

IEEE/ACM TRANSACTIONS ON

COMPUTATIONAL BIOLOGY AND BIOINFORMATICS

IEEE Computer Society Publishing Services Staff

ALICIA L. STICKLEY, *Senior Manager, Publishing Services*
PILAR HAWTHORNE, *Senior Transactions Production Editor*
STEVE WAREHAM, *Digital Production Supervisor*
MARK J. BARTOSIK, *Lead Digital Production Specialist*
HILDA CARMAN, *Manager of Administrative Services*
KATHLEEN HENRY, *Publications Coordinator*

IEEE/ACM TRANSACTIONS ON COMPUTATIONAL BIOLOGY AND BIOINFORMATICS is published bimonthly by the IEEE Computer Society. **IEEE Corporate Office:** Three Park Avenue, 17th Floor, New York, NY 10016-5997 USA. Responsibility for the content rests upon the authors and not upon the IEEE/ACM or the IEEE Computer Society. **IEEE Computer Society Publications Office:** 10662 Los Vaqueros Circle, Los Alamitos, CA 90720 USA. **IEEE Computer Society Headquarters:** 2001 L Street N.W., Suite 700, Washington, DC 20036-4928 USA. **Back issues:** IEEE members or members of financial cosponsors $20.00, nonmembers $92.50 per copy. (Note: Add $4.00 postage and handling charge to any order from $1.00 to $50.00, including prepaid orders). Complete price information available on request. **Reuse Rights and Reprint Permissions:** Educational or personal use of this material is permitted without fee, provided such use: 1) is not made for profit; and 2) includes this notice and a full citation to the original work on the first page of the copy; and 3) does not imply IEEE endorsement of any third-party products or services. Authors and their companies are permitted to post their IEEE-copyrighted material on their own web servers without permission, provided that the IEEE copyright notice and a full citation to the original work appear on the first screen of the posted copy. Permission to reprint/republish this material for commercial, advertising or promotional purposes or for creating new collective works for resale or redistribution must be obtained from IEEE by writing to the IEEE Intellectual Property Rights Office, 445 Hoes Lane, Piscataway, NJ08854-4141 or pubs-permissions@ieee.org . Copyright © 2013 IEEE. All rights reserved. Abstracting and Library Use: Abstracting is permitted with credit to the source. Libraries are permitted to photocopy for private use of patrons, provided the per-copy fee indicated in the code at the bottom of the first page is paid through the Copyright Clearance Center, 222 Rosewood Drive, Danvers, MA 01923. Periodicals postage paid at New York, NY, and at additional mailing offices. **Postmaster:** Send address changes to IEEE/ACM TRANSACTIONS ON COMPUTATIONAL BIOLOGY AND BIOINFORMATICS, IEEE Service Center, 445 Hoes Lane, PO Box 1331, Piscataway, NJ 08854-4141 USA. GST Registration No. 125634188. Canada Post Publications Mail Agreement Number 40013885. Return Undeliverable Canadian Addresses to: PO Box 122, Niagara Falls, ON L2E 6S8. Printed in the USA on ANSI/NISO standard Z39.48-1992 acid-free paper.

IEEE/ACM *TCBB*

tcbb@computer.org
www.computer.org/tcbb

(Contents continued from back cover)

ABOUT THE COVER IMAGE: Plot of clustering results using GDHC with average linkage. The tree was cut using dynamic tree cutting with a limit of minimum cluster size of 50. Indicator of periodic genes (right): blue indicate the gene was identified as periodic gene using Fisher's exact g test for periodicity [38]. The three columns represent the three cell cycle data sets. Image courtesy of Tianwei Yu and Hesen Peng, Department of Biostatistics and Bioinformatics, Emory University, Atlanta. See article, pages 1080-1085.

For manuscript submission information, please see our guidelines detailed at the *TCBB* author center, www.computer.org/portal/web/tcbb/author.

Designing Template-Free Predictor for Targeting Protein-Ligand Binding Sites with Classifier Ensemble and Spatial Clustering

Dong-Jun Yu, Jun Hu, Jing Yang, Hong-Bin Shen, Jinhui Tang, and Jing-Yu Yang

Abstract—Accurately identifying the protein-ligand binding sites or pockets is of significant importance for both protein function analysis and drug design. Although much progress has been made, challenges remain, especially when the 3D structures of target proteins are not available or no homology templates can be found in the library, where the template-based methods are hard to be applied. In this paper, we report a new ligand-specific template-free predictor called TargetS for targeting protein-ligand binding sites from primary sequences. TargetS first predicts the binding residues along the sequence with ligand-specific strategy and then further identifies the binding sites from the predicted binding residues through a recursive spatial clustering algorithm. Protein evolutionary information, predicted protein secondary structure, and ligand-specific binding propensities of residues are combined to construct discriminative features; an improved AdaBoost classifier ensemble scheme based on random undersampling is proposed to deal with the serious imbalance problem between positive (binding) and negative (nonbinding) samples. Experimental results demonstrate that TargetS achieves high performances and outperforms many existing predictors. TargetS web server and data sets are freely available at: http://www.csbio.sjtu.edu.cn/bioinf/TargetS/ for academic use.

Index Terms—Protein-ligand binding sites, ligand-specific prediction model, template-free, classifier ensemble, spatial clustering

1 Introduction

Protein-ligand interactions are indispensable for biological activities and play important roles in virtually all biological processes [1], [2], [3]. Hence, accurately identifying the protein-ligand binding sites or pockets is of significant importance for both protein function analysis and drug design [4]. Much effort has been made to reveal the intrinsic mechanism of protein-ligand interactions and thousands of protein-ligand complexes have been deposited into protein data bank (PDB) [5]. Due to the importance of protein-ligand interactions and the difficulty of experimentally identifying of protein-ligand binding sites, developing computational methods for the prediction of protein-ligand binding sites using sequence and/or structural information has become a hot spot in recent bioinformatics research [6], [7], [8].

There have emerged many computational methods for predicting protein-ligand binding sites during the past decades [8], [9], [10], [11] and various algorithms for identifying protein-ligand binding sites in proteins have been comprehensively reviewed and explained in detail by Leis et al. [8] and Laurie and Jackson [11]. Roughly speaking, these existing methods can be grouped into three categories according to the features they used [12]: structure-based methods, sequence-based methods, and hybrid methods that utilize both the structural and sequence information.

In the early stage, structure-based methods dominate in the fields of protein-ligand binding sites prediction. To name a few: LIGSITE [13], CASTp [14], SURFNET [15], POCKET [16], fpocket [17], Q-SiteFinder [18], SITEHOUND [19], and so on. Often, these structure-based predictors try to utilize the protein 3D information and appropriate geometry measurements to locate the potential binding sites (pockets). For example, in LIGSITE [13], a regular 3D grid is placed around the protein; then, lines are drawn from each grid point along the x-, y-, z-axis as well as the cubic diagonals of the grid; segments of lines that are enclosed by protein from both sides are considered as pockets [8]. In the CASTp [14], alpha shape theory and triangulation methods are used to predict pockets: a Delaunay triangulation of the protein is first performed; then, based on the direction of norm vectors associated with triangles for a set of neighboring triangles, a potential pocket can be detected. Most structure-based methods relay on the assumption that proteins binding similar ligands have similar overall structural or biochemical properties. However, researchers have found proteins that do not display any overall sequence or structure similarity may also present similar binding sites [20]. Therefore, local comparison of binding pockets is a more appropriate approach to predict if two proteins bind similar ligands [21]. For example, Hoffmann et al. [20] proposed a method to quantify the similarity between binding pockets, based on which they can predict binding ligands for a given target pocket by comparing it to an ensemble of pockets with known ligands.

- *D.J. Yu, J. Hu, J. Tang and J.Y. Yang are with the School of Computer Science and Engineering, Nanjing University of Science and Technology, 200 Xiaolingwei Road, Nanjing 210094, China. E-mail: njyudj@njust.edu.cn.*
- *J. Yang and H.B. Shen are with the Institute of Image Processing and Pattern Recognition, Shanghai Jiao Tong University, and Key Laboratory of System Control and Information Processing, Ministry of Education of China, Shanghai 200240, China. E-mail: jay516@163.com, hbshen@sjtu.edu.cn.*

Manuscript received 12 Mar. 2013; revised 3 June 2013; accepted 5 Aug. 2013; published online 19 Aug. 2013.
For information on obtaining reprints of this article, please send e-mail to: tcbb@computer.org, and reference IEEECS Log Number TCBB-2013-03-0077. Digital Object Identifier no. 10.1109/TCBB.2013.104.

Whereafter, researchers found that features derived from protein sequences can also be effectively used for protein-protein interfaces and protein-ligand binding sites prediction. For example, ConSurf [22] and Rate4Site [23] use the evolutionary data derived from multiple-sequence alignment technique to identify hot spots and surface patches that are likely to be in contact with other proteins, domains, peptides, DNA, RNA, or other ligands; L1pred [24] predicts catalytic residues in enzymes by using the L1-logreg classifier to integrate eight sequence-based scoring functions.

Recently, considerable attention has been paid to the methods that combine both the structural and sequential information to further improve prediction accuracy of protein-ligand binding sites. For example, LIGSITE^{csc} [25] extends the LIGSITE [13] by incorporating the degree of conservation of the involved surface residues, ConCavity [26] integrates evolutionary sequence conservation estimates with structure-based methods for identifying protein surface cavities, and SURFNET-ConSurf [27] also incorporates residue evolutionary conservation into pocket detection.

Although much progress has been made in computational methods for protein-ligand binding sites prediction and many applications based on these methods have emerged, there still exist several issues deserved to be further investigated:

First, many structure-based methods are template-based that require tertiary protein structures as inputs to search for existing well-characterized proteins as templates for homology comparative prediction [9], [10], [28], [29]. However, on the one hand, it is very common in many realistic scenarios (e.g., drug design project) where a given protein target only has sequence information and no corresponding 3D structure is available [8], thus the applicability of these structure-based methods will be limited. On the other hand, these template-based methods will also fail to perform novel predictions for features absent in the template library [2]. These are two of the major reasons that motivate researchers in this field to develop useful methods for predicting protein-ligand binding sites from the protein sequence information alone.

Second, a common drawback of most existing sequence-based protein-ligand binding prediction methods (e.g., ATPsite [7] and NsitePred [30] for ATP binding residue prediction; DiANNA [31] for ternary cysteine prediction: discriminating between free, metal binding, disulphide binding for cysteines [32], etc.) is that they are *bonding state prediction* [33], i.e., they can only predict the protein-ligand binding residues from sequences and cannot tell which residues may potentially form the binding sites (pockets). It is believed that a deep understanding of the mechanism of protein-ligand interaction requires more than this simple two-state or three-state prediction and thus developing effective methods for further identify the binding sites (pockets) from the predicted binding residues is necessary.

Third, most of the aforementioned methods focused on predicting *general-purpose* ligand binding sites without carefully considering the differences between various ligands. In fact, protein binding sites vary significantly in their roles, sizes, and distributions for different types of protein-ligand interactions and different ligands tend to binding to different residues with specificities [34], [35]. Considering the significant difference between different types of ligands, developing ligand-specific binding sites predictor has attracted considerable attentions to obtain much more accurate predictions, and many ligand-specific binding sites predictors have emerged recently [36]. For example, Liu et al. developed HemeNet [37] and HemeBIND [12] for specifically predicting HEME binding residues based on structural and sequential information, Sodhi et al. [38] exploited neural network methods to predict metal ions binding sites, Brylinski and Skolnick [39] extended the FINDSITE software to FINDSITE-metal for specifically predicting metal ions binding sites, and Kumar et al. [40] developed Pprint, an RNA binding site predictor using SVM and PSSM profile; several predictors specifically designed for Adenosine-5′-triphosphate (ATP) binding residues prediction have also been released [6], [7], [30] recently. In this study, we will experimentally demonstrate that ligand-specific binding sites predictor is better than *general-purpose* ligand binding sites predictor and really helps to further improve prediction accuracy.

In view of the above-mentioned three important issues, we thus developed a ligand-specific template-free protein-ligand binding sites predictor, called TargetS, which currently can predict binding sites for 12 types of ligands and is flexible to incorporate prediction modules for other new types of ligands. Protein conservation matrix, predicted protein secondary structure matrix, and ligand-specific binding propensities of residues are combined to extract discriminative features; classifier ensemble with SVM [41], [42] as base classifier and random undersampling technique are integrated to tackle the serious imbalance phenomenon between negative and positive samples (i.e., nonbinding and binding residues). TargetS performs prediction task with a two-stage scheme: In the first stage, it predicts which residues are protein-ligand binding residues with ligand-specific prediction modules, while in the second stage, the predicted binding residues are spatially clustered into the binding sites (pockets) according to the protein 3D structures either provided by the user or modeled by the MODELLER software [43]. The TargetS is freely accessible at http://www.csbio.sjtu.edu.cn/bioinf/TargetS/ for academic use.

2 Materials and Methods

2.1 Benchmark Data Sets

Most ligand-binding sites prediction methods use the protein structures from the PDB [44] as templates [45]. However, not all ligands present in the PDB are biologically relevant, as small molecules are often used as additives for solving the protein structures [46], [47]. Much effort has been made to filter out the biologically ligand-protein interaction from the PDB and several purified ligand-protein interaction data sets have appeared, such as FireDB [47], LigASite [46], PDBbind [48], and BioLip [45], among which BioLip is the most recently released semimanually curated database for biologically relevant ligand-protein interactions. BioLip was constructed by a four-step biological feature filtering procedure followed by careful manual verifications [45]: First, an automated four-step hierarchical procedure is used to verify the biological relevance of a ligand. After the

TABLE 1
Composition of the Training Data Sets and the Independent Validation Data Sets for the 12 Types of Ligands

Ligand Category	Ligand Type	Training Dataset		Independent Validation Dataset		Total No. of Sequences
		No. of Sequences	(numP, numN)*	No. of Sequences	(numP, numN)*	
Nucleotide	ATP	221	(3021, 72334)	50	(647, 16639)	271
	ADP	296	(3833, 98740)	47	(686,20327)	343
	AMP	145	(1603, 44401)	33	(392, 10355)	178
	GDP	82	(1101, 26244)	14	(194, 4180)	96
	GTP	54	(745, 21205)	7	(89, 1868)	61
Metal Ion	Ca^{2+}	965	(4914, 287801)	165	(785,53779)	1130
	Zn^{2+}	1168	(4705, 315235)	176	(744, 47851)	1344
	Mg^{2+}	1138	(3860, 350716)	217	(852, 72002)	1355
	Mn^{2+}	335	(1496, 112312)	58	(237, 17484)	393
	Fe^{3+}	173	(818, 50453)	26	(120, 9092)	199
	DNA	335	(6461, 71320)	52	(973, 16225)	387
	HEME	206	(4380, 49768)	27	(580, 8630)	233

** Figures numP, numN in 2-tuple (numP, numN) represent the numbers of positive (binding residues) and negative (non-binding residues) samples, respectively.*

automated procedure is completed, a careful manual check is performed to eliminate possible false positives, which can occur for entries with the commonly used crystallization additives. By doing so, it is believed with high confidence that the ligand-protein interactions collected from PDB are real biologically relevant. Details for constructing BioLip can be found in [45].

To evaluate the effectiveness of the proposed TargetS, we thus constructed training data sets and independent validation data sets based on the BioLip [45] rather than on PDB. Twelve different types of ligands, i.e., five types of metal ions, five types of nucleotides, DNA, and HEME, were considered in this study. For each of the 12 types of the considered ligands, we constructed its training data set and independent validation data set as follows:

Training data sets. We extracted all the protein sequences, which interact with the given ligand and were released into PDB before 10 March 2010, from BioLip, and then the maximal pairwise sequence identity of the extracted protein sequences was culled to 40 percent with PISCES software [49] and the resulting sequences constitute the training data set for that ligand.

Independent validation data sets. We extracted all the protein sequences that interact with the ligand and were deposited into PDB after 10 March 2010 from BioLip. Again, the maximal pairwise sequence identity of the extracted protein sequences was reduced to 40 percent and the resulting sequences constitute the validation data set. Moreover, if a given sequence in the validation data set shares $>40\%$ identity to a sequence in the training data set, then we remove the sequence from the validation data set. This assures that the sequences in validation data set are independent of those in training data set. Table 1 summarizes the detailed compositions of the training data sets and the independent validation data sets for the 12 types of ligands.

To further demonstrate the effectiveness of the proposed TargetS, CASP9 data set was used for blind test. The ninth community-wide critical assessment of techniques for protein structure prediction (CASP9) released 129 target protein sequences for blind test of protein structure and function prediction methods. Among the 129 sequences, 31 were used for evaluating the ligand binding-site predictions, where the predictors were asked to identify ligand binding residues in the sequences. As one sequence (Target ID: T0533) was canceled on 26 May 2010, the remaining 30 sequences were, thus, taken as targets for our consideration.

It has not escaped from our notice that the percentages of binding residues in training and validation data sets for a given ligand are different. However, this difference will not affect the objective evaluation procedure of the proposed method as we performed both the cross-validation evaluation on training data set and the independent test on the testing data set. The purpose of the cross-validation is to evaluate the overall performance of the proposed method on a given data set. While independent test is often used to evaluate the generalization capability of the proposed method, which has been widely accepted in this field.

2.2 Feature Extraction

2.2.1 Position Specific Scoring Matrix Feature

Position specific scoring matrix (PSSM) well encodes the evolutionary information of a protein sequence. Tremendous previous studies have shown its prominent discriminative capability for many prediction problems in bioinformatics, such as protein function prediction [50], protein-ATP binding sites prediction [51], transmembrane helices prediction [52], protein secondary structure prediction [53], subcellular localization prediction [54], [55], [56], and so on.

The position specific scoring matrix for protein sequence is built by using the PSI-BLAST [57] to search the Swiss-Prot database through three iterations with 0.001 as the e-value cutoff for multiple sequence alignment against the query

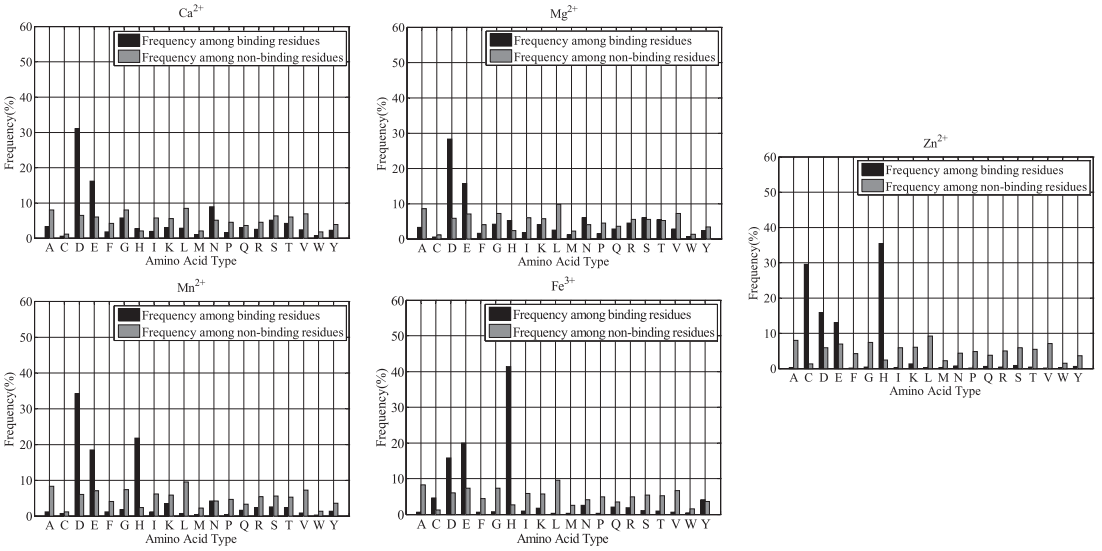

Fig. 1. Frequencies of the 20 native amino acids among binding and nonbinding residues for Ca^{2+}, Mg^{2+}, Mn^{2+}, Fe^{3+}, and Zn^{2+}.

sequence. The obtained PSSM is further normalized with the logistic function:

$$f(x) = \frac{1}{1 + \exp(-x)}, \quad (1)$$

where x is the original score in PSSM matrix. Then, a sliding window of size W is applied to each residue to extract its PSSM feature vector. In this study, we have tested different values of W and found that $W = 17$ is a better choice. Thus, the dimensionality of PSSM feature vector is $17 \times 20 = 340$.

2.2.2 Predicted Protein Secondary Structure Feature

Previous studies have shown that there exists close relationship between protein structures and functionalities. Many structural characteristics related to identification of critical residues (e.g., ligand-binding residues) have been intensively investigated, such as the secondary structure information and so on. [51], [58]. The predicted secondary structure information of a protein sequence is obtained by applying PSIPRED [59] software, which predicts the probabilities of belonging to three secondary structure classes (coil (C), helix (H), and strand (E)) for each residue in a protein sequence. More specifically, for a protein sequence with L residues, the PSIPRED outputs an $L \times 3$ probability matrix, which represents the predicted secondary structure information of the protein. Again, a sliding window of size 17 was used to extract protein secondary structure feature, denoted as PSS, of each reside and the dimensionality of the extracted PSS feature is $17 \times 3 = 51$.

2.2.3 Ligand-Specific Binding Propensity Feature

Previous studies have shown that different ligands tend to bind different types of residues and this binding propensity may potentially help to improve the binding sites prediction accuracy [34], [35]. For example, Gromiha and Fukui [60] analyzed the binding propensity among protein-DNA complexes and found that positively charged, polar, and aromatic residues are important for binding. In light of this, we will also incorporate binding propensity feature in our method.

We calculated the frequencies of the 20 native amino acids among binding residues for each type of ligands and found that the ligands clearly has binding propensity. Taking metal ion ligands as example, for each of the five considered metal ion ligands, we calculated and plotted the frequencies of the 20 native amino acids among binding and nonbinding residues, as shown in Fig. 1. By observing Fig. 1, several observations can be drawn:

First, each type of metal ion ligands favors to bind some specific types of residues. For example, ASP (D), GLU (E), ASN (N), and GLY (G) are the top four types of residues to which Ca^{2+} tends to bind, while HIS (H), CYS (C), ASP (D), and GLU (E) are the top four types of residues which will more often coordinate the Zn^{2+}. This observation agrees with the arguments obtained by other researchers such as Lu et al. [61]. Second, some types of residues will always appear with high frequencies for different types of metal ion-binding residues. It is easy to find that the resiude ASP (D), and GLU (E) consistently appear with high frequencies among all the five types of metal ion-binding residues. These statistical results inspired us that the binding propensities of residues can be utilized as effective indexes to guide the identification process of protein-ligand binding. Together with the fact that the binding propensities of a same residue differ significantly for different ligands, we thus extract ligand-specific 17D binding propensity feature vector for each residue in a protein sequence by concatenating the binding propensities of its neighboring residues within the window of size 17 centered at the residue.

2.3 Application of Machine Learning Methods

Protein-ligand binding prediction is a typical imbalanced learning problem, i.e., the numbers of samples in different classes (binding or nonbinding) differ significantly. Directly applying the traditional statistical machine learning algorithms, which assume that samples in different classes are balanced, to imbalanced problems often leads to a poor performance [62]. To circumvent this problem, random undersampling technique is taken [63] to alter the size of the majority class by randomly removing samples from the

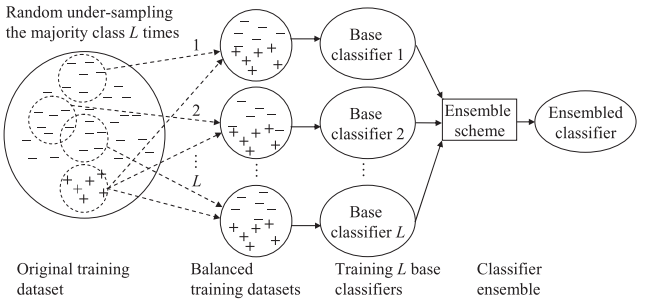

Fig. 2. Architecture of the classifier ensemble procedure based on random undersampling technique. "+" denotes a sample in the minority class, while "−" denotes a sample in the majority class.

majority class. Random undersampling can provide a parsimonious training data set because it removes samples from the original data set. However, part of the important information buried in the removed samples may also be lost simultaneously. We, thus, exploited the method of combing multiple undersamplings with classifier ensemble to perform protein-ligand binding prediction: first, we sample L different majority training subsets by random undersampling the majority class L times; then, we train a base classifier on each of the majority training subsets plus the minority training set. By doing so, on the one hand, merits derived from undersampling such as sample balance can be retained. On the other hand, multiple samplings can reduce the loss of information caused by random undersampling to some extent, thus may potentially provide better prediction performance. Finally, the trained base classifiers are ensembled by an appropriate ensemble scheme to perform the final decision. Fig. 2 illustrates the architecture of the classifier ensemble procedure based on random undersampling technique. In this study, support vector machine (SVM) [41], [42] was used as base classifier.

The next key problem is how to achieve best final decision from the outputs of the L base classifiers with an effective ensemble scheme. Classifier ensemble has been widely applied in bioinformatics, such as prediction of all-alpha membrane proteins [64], protein fold prediction [65], [66], protein subcellular localization prediction [54], and protein structural class prediction [67] and so on. However, ensemble scheme are problem-dependent and the theoretical justification for choosing is still unavailable. In view of this, in this study, we have tested several popular ensemble schemes including *Maximum* ensemble, *Minimum* ensemble, *Mean* ensemble, *Dempster-Shafer* ensemble [68], *AdaBoost* ensemble [69], and *Decision Template* ensemble [70]. The best one, i.e., *AdaBoost*, was finally chosen.

The idea of *AdaBoost* ensemble is to develop the classifier team $S^E = \{S_1^E, S_2^E, \ldots, S_k^E, \ldots, S_K^E\}$ by incrementally selecting one base classifier each time from the base classifier pool $S = \{S_1, S_2, \ldots, S_i, \ldots, S_L\}$, $K \leq L$ and $S_k^E \in S$. The base classifier S_i that joins the ensemble at step i is trained on a training subset selectively sampled from the training data set $X^{Tr} = \{\mathbf{x}_t^{Tr}\}_{t=1}^N$ by applying a sample-distribution-based sampling technique. Details for *AdaBoost* could be found in [69] or [70].

However, two reasons motivate us to develop a modified *AdaBoost* ensemble scheme, denoted as *MAdaBoost*, rather than utilizing the traditional *AdaBoost* ensemble directly:

1. In the traditional *AdaBoost*, samples (binding residues and nonbinding residues in this study) in the whole training data set are used as evaluation samples to calculate the ensemble error of each base classifier. In other words, evaluation samples and training samples originate from the same protein sequence thus having high homology, which will lead to an overoptimistic performance on training data while having poor generalization performance on the testing data. In view of this, we will utilize and independent evaluation data set, among which samples have low homology with those in training data set, to facilitate the ensemble procedure. How to choose the independent evaluation data set will be described subsequently.
2. To reduce the impact of the serious imbalance between positive (binding) and negative (nonbinding) samples, we will still use random undersampling technique to balance samples for training the base classifiers during the ensemble procedure.

Let $\Omega = \{\omega_1, \omega_2, \ldots, \omega_C\}$ be the set of classes, $S = \{S_1, S_2, \ldots, S_L\}$ be the set of L base classifiers which are trained on a corresponding data set randomly undersampled from training data set $X^{Tr} = \{\mathbf{x}_t^{Tr}\}_{t=1}^N$. For a given input sample $\mathbf{x}$, the ith base classifier S_i outputs a C-dimensional vector $S_i(\mathbf{x}) = (s_{i,1}(\mathbf{x}), s_{i,2}(\mathbf{x}), \ldots, s_{i,j}(\mathbf{x}), \ldots, s_{i,C}(\mathbf{x}))^T$, where $s_{i,j}(\mathbf{x})$ measures the probability of $\mathbf{x}$ being classified into class j, $1 \leq j \leq C$. Let $X^{Eval} = \{\mathbf{x}_t^{Eval}\}_{t=1}^M$ be the independent evaluation data set, the two-tuple $(S^E, \{\varepsilon_k^E\}_{k=1}^K)$ be the ensembled results, where $S^E = \{S_1^E, S_2^E, \ldots, S_k^E, \ldots, S_K^E\}$ consists of the base classifiers selected from the base classifier pool and ε_k^E is the corresponding weighted ensemble error of the kth selected base classifier. Then, the flowchart of the proposed modified *AdaBoost* (*MAdaBoost*) procedure can be illustrated in Fig. 3.

We use V-fold cross-validation to evaluate the performance of the proposed *MAdaBoost* ensemble as follows:

First, we randomly partition the sequences rather than the residues of sequences in the original training data set into V disjoint subsets. By partitioning the original training data set on sequence rather than residue level, the low homology between evaluation samples and training samples during ensemble procedure can be guaranteed.

Second, residues of sequences in one subset constitute the testing data set X^T in the current round of cross validation, residues of sequences in one subset are used to construct independent evaluation data set X^{Eval}, and the residues of sequences in the remaining V-2 subsets are used as training data set X^{Tr}. X^{Tr} and X^{Eval} are then used for classifier ensemble with the *MAdaBoost* ensemble scheme (see Fig. 3). After classifier ensemble, samples in X^T are fed to the ensembled classifier $(S^E, \{\varepsilon_k^E\}_{k=1}^K)$ to obtain their probability outputs: for a sample $\mathbf{x}$ in X^T, its support for class ω_j $(1 \leq j \leq C)$ obtained from the ensembled classifier $(E, \{\varepsilon_k^E\}_{k=1}^K)$ is formulated as

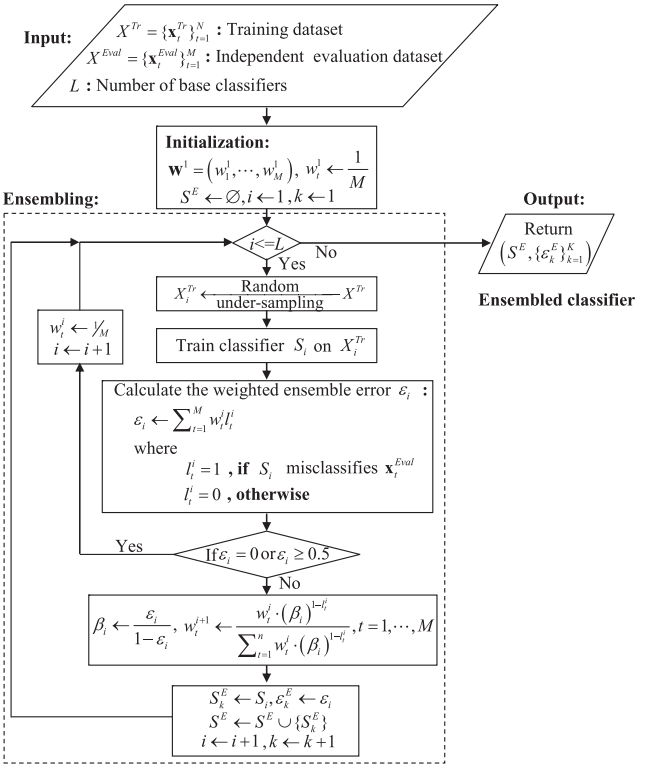

Fig. 3. Flowchart of the proposed modified AdaBoost (MAdaBoost).

$$\mu_j(\mathbf{x})=\sum\nolimits_{1\leq k\leq K,\ \mathrm{label}(S_k^E(\mathbf{x}))=\omega_j}\left(1-\varepsilon_k^E\right)\times s_{k,j}^E(\mathbf{x})+\sum\nolimits_{1\leq k\leq K,\ \mathrm{label}(S_k^E(\mathbf{x}))\neq\omega_j}\varepsilon_k^E\times s_{k,j}^E(\mathbf{x}),\tag{2}$$

where ε_k^E is the weighted ensemble error of the base classifier k in the ensembled classifier team, $S_k^E(\mathbf{x})=(s_{k,1}^E(\mathbf{x}),s_{k,2}^E(\mathbf{x}),\ldots,s_{k,i}^E(\mathbf{x}),\ldots,s_{k,C}^E(\mathbf{x}))^T$, $\mathrm{label}(S_k^E(\mathbf{x}))=\omega_j$ means that the input $\mathbf{x}$ is classified into class ω_j by the kth base classifier $S_k^E(\mathbf{x})$ in the ensembled classifier team, i.e., the jth component of the output of the classifier S_k^E under the input $\mathbf{x}$ is maximal:

$$j=\arg\max_i\ s_{k,i}^E(\mathbf{x}),1\leq i\leq C.\tag{3}$$

Third, this practice continued until all the V subsets of the original training data set are traversed over for testing.

After V-fold cross-validation, the probabilities of being binding residues of all the residues in the original training data set can be obtained. Further, the prediction performance of proposed method on training data set over V-fold cross-validation can be calculated by setting a threshold, i.e., residues with probabilities above the threshold are marked as ligand binding residues, while those ones with probabilities less than the threshold are marked as non-binding residues. How to choose the threshold T for reporting the performance will be described in the experimental results section.

2.4 Clustering Binding Residues to Binding Site(s)

As stated in Section 1, most of the existing sequence-based protein-ligand binding predictors can only perform *bonding state* prediction, i.e., they can only predict protein-ligand binding residues rather than binding sites from sequences. In fact, it will be more useful for biologists and users if the predictor can tell which binding residues actually form a binding site (pocket), especially in the situation where there exist more than one binding sites (pockets) in one protein sequence.

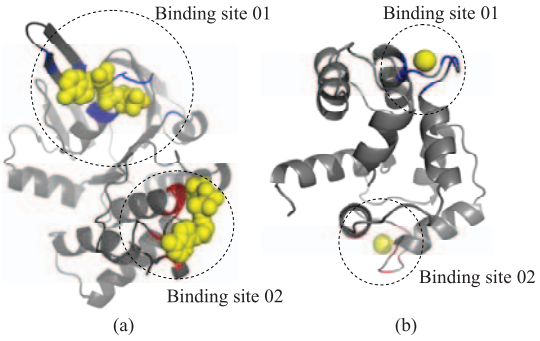

Fig. 4. Visualization of protein-ligand binding sites. (a) illustrates the protein 1L2TA, which interacts with two ATP ligands; while (b) illustrates the protein 1A29A, which interacts with two Ca^{2+} ligands.

Previous studies have shown that residues located in protein-ligand binding interfaces tend to form spatial clusters [71]. Taking chain A of protein 1L2T (interacts with ligand ATP) and chain A of protein 1A29 (interacts with ligand Ca^{2+}) as examples, we drew their 3D structures with cartoon representation as shown in Fig. 4, where the blue and red residues are observed ligand-binding residues, and ligands (ATP and Ca^{2+}) are highlighted in yellow color. From Fig. 4, it is easy to find that the residues colored in blue and red are spatially clustered and form binding sites 01 and 02, respectively, for both proteins.

Based on this observation, we thus have developed a *r*ecursive *s*patial *c*lustering *p*rocedure, denoted as *RSCP*, which has been demonstrated effective in our recent work for protein-ATP binding site prediction [72], to further identify which of the predicted binding residues may potentially form binding site(s).

Let *PBR* be the set of the *p*redicted *b*inding *r*esidues for a given protein, T_{ligand} be the ligand-specific threshold for spatial clustering, and P_{3D} be the 3D structure (predicted or observed) of the protein. Then, the predicted binding residues in PBR can be clustered into *p*redicted *b*inding *s*ites, denoted as *PBS*, using the following recursive spatial clustering procedure, as shown in Fig. 5.

Note that in the spatial clustering procedure, the clustering threshold T_{ligand} is ligand-dependent and dominates how many clusters (binding sites) will be obtained after spatial clustering. Obviously, a large T_{ligand} will produce small number of clusters, while a small T_{ligand} will lead to a large number of clusters. Thus, how to set an appropriate T_{ligand} is crucial for the spatial clustering procedure. In this study, the ligand-dependent clustering threshold T_{ligand} was obtained as follows: For each type of ligand, we performed spatial clustering procedures on the observed binging residues in the corresponding training data set for that ligand with different clustering thresholds (T_{ligand}) by varying the values of T_{ligand} from 10 (Å) to 100 (Å) with a step size of 0.5 (Å), and the one which maximizes the *clustering accuracy* was chosen as the final threshold for that ligand.

Two measures were used to evaluate the performance of clustering algorithm and optimize the clustering parameters

Procedure	*PBS=RSCP(PBR,T_{ligand},P_{3D})*
Input	*PBR*: The set of predicted ligand-binding residues; T_{ligand}: Threshold for spatial clustering; P_{3D}: 3D structure (predicted or observed) of the protein.
Output	*PBS*: A set of clusters, residues in each cluster constitute a binding site.
1	Calculate the *max_distance*: the maximal distance between any two residues in *PBR*.
2	**IF** *max_distance* is greater than the pre-defined threshold T_{ligand}
	2.1 Clustering the residues in *PBR* into two smaller clusters according to their spatial positions with standard *K*-means algorithm: PBR_1 and PBR_2
	2.2 PBS_1=*RSCP* (PBR_1, T_{ligand}, P_{3D})
	2.3 PBS_2=*RSCP* (PBR_2, T_{ligand}, P_{3D})
	2.4 $PBS=PBS_1 \cup PBS_2$
	ELSE
	2.5 *PBS=PBR*
	END IF
3	**RETURN** *PBS*

Fig. 5. Spatial clustering procedure for clustering binding residues to binding sites.

on the training data sets. The first measure is V_{site}, which measures the percentage of the observed binding sites that have been correctly clustered. In this study, an observed binding site is considered to be correctly clustered if its 90 percent binding residues are included in the clustered binding site. The second measure is V_p, which measures the percentage of proteins in the training data set that have been correctly clustered. A protein is considered being correctly clustered if all the binding sites in this protein are correctly clustered and the number of the clustered binding sites is equal to the number of the observed binding sites in the protein. Table 2 lists the optimal clustering thresholds for the 12 types of ligands after performing the above-mentioned empirical evaluations on their corresponding training data sets. As we can see that generally the larger of the ligand, the bigger of the threshold will be.

2.5 Designing Ligand-Specific Prediction Model

Many existing protein-ligand prediction methods focused on predicting general ligand binding sites without carefully considering the differences in various ligands [12]. In fact, protein-ligand binding sites vary significantly in their roles, sizes, and distributions for different types of protein-ligand interactions [34]. For example, we calculated that the averaged diameter of nucleotide ligands is about 22 Å, while the averaged diameter of metal ion ligands is only about 2 Å. We also calculated the averaged size of binding site (averaged number of residues in each binding site/pocket) for the 12 types of considered ligands as listed in Table 3. It is easy to find that the averaged size of binding site differs significantly between different ligand categories. For example, the averaged size of binding site for nucleotide category (ATP, AMP, ADP, GDP, and GTP) is about 12, while the averaged size of binding site for metal ion category (Ca^{2+}, Mg^{2+}, Mn^{2+}, Fe^{3+}, and Zn^{2+}) is only about 3, the difference between them is approximately 9; on the other hand, the averaged sizes are similar among the same ligand category. Taking metal ion category as an example, the maximal and minimal averaged sizes of the five considered ligands are 2.95 and 3.80, respectively, and the difference is only about 0.85. Similar phenomenon can also be found in nucleotide category. In addition, different ligands (e.g., Ca^{2+}, Mg^{2+}, Mn^{2+}, Fe^{3+}, and Zn^{2+}) are also found to tend to bind different residues even if they belong to the same ligand category (e.g., metal ion) which we have discussed in Section 2.2.

TABLE 2
Thresholds for Spatial Clustering Procedure of the 12 Types of Ligands

Ligand Type	ATP	AMP	ADP	GDP	GTP	Ca^{2+}	Zn^{2+}	Mg^{2+}	Mn^{2+}	Fe^{3+}	DNA	HEME
T_{ligand} (Å)	27.5	29.0	27.5	23.0	26.0	19.0	19.0	20.0	19.0	19.0	61.0	33.0

TABLE 3
Averaged Size of Binding Site for the 12 Types of Ligands

Ligand Type	ATP	AMP	ADP	GDP	GTP	Ca^{2+}	Zn^{2+}	Mg^{2+}	Mn^{2+}	Fe^{3+}	DNA	HEME
Averaged Size	12.69	10.21	12.34	12.82	12.17	3.73	3.07	2.95	3.41	3.80	11.73	16.65

In view of the above observations, we believe and will demonstrate that developing ligand-specific protein-ligand binding sites predictor, i.e., designing a specific model for each type of ligands, may help to further improve the prediction accuracy.

2.6 Workflow of the Proposed Predictor

We designed and implemented a ligand-specific template-free predictor for targeting protein-ligand binding sites, called TargetS, with modular design strategy to facilitate it with good flexibility and scalability. Fig. 6 illustrates the workflow of the proposed TargetS.

The TargetS server accepts two different types of query protein information for protein-ligand binding sites prediction: one is protein sequence in FASTA format; the other is standard PDB file format, which contains 3D structure information of a protein. Note that if the user inputs a PDB file, corresponding sequence will be picked out from the PDB file for subsequent sequence-based feature extraction (e.g., PSSM and PSS). For each protein (sequence or PDB file) submitted from the client, the server performs binding sites predictions for different types of ligands the user designated by using corresponding ligand-specific prediction models. Note that if the user designate "I don't know the ligand types," the TargetS will perform predictions for all the 12 types of ligands, respectively. For each type of ligand, TargetS accomplishes the prediction task with a two-stage scheme: In the first stage, the server predicts which residues are binding residues, while in the second stage, the server further identifies binding sites from the predicted binding residues with spatial clustering algorithm.

Note that if the user submits a PDB file, then the residues' 3D coordinates contained in the PDB file can be directly utilized for spatial clustering. If the user only submits a protein sequence, the 3D structure of the query

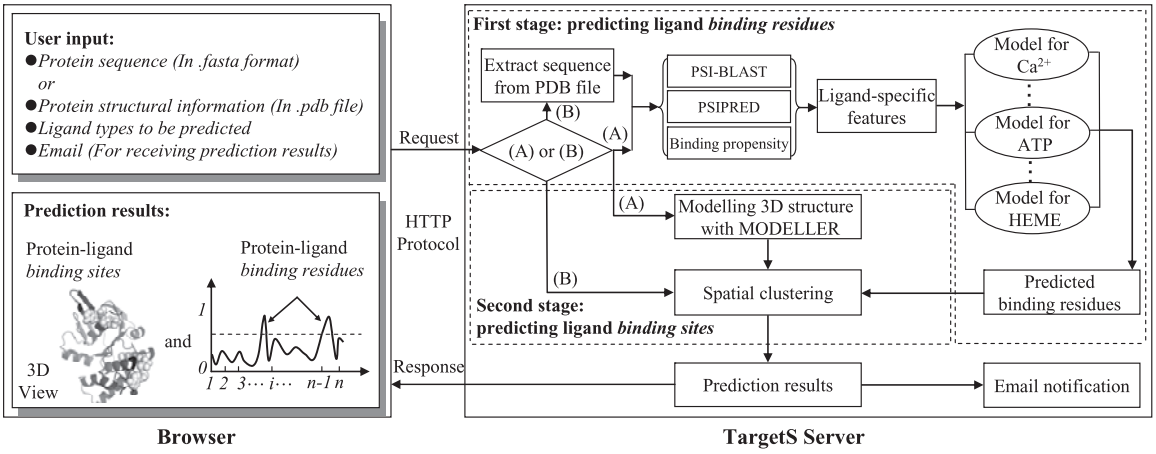

Fig. 6. Workflow of the proposed TargetS. (A) denotes that the user submits protein sequence, and (B) denotes that the user submits a PDB file. MODELLER [41] is a software package for predicting 3D structure from protein sequence.

sequence will be first modeled by applying MODELLER [43] software package, and then the predicted 3D structure is used for spatial clustering.

After the two-stage prediction, TargetS returns the prediction results back to the client in two different ways: online real-time feed back with 3D illustrations and text descriptions, and an independent e-mail notification to the e-mail address (optional) provided by the user.

3 Experimental Results and Discussions

Specificity (*Spe*), *Sensitivity* (*Sen*), *Accuracy* (*Acc*), and the *Matthews correlation coefficient* (*MCC*) were used to evaluate the performance of the proposed methods as follows:

$$Specificity = \frac{TN}{TN + FP}, \tag{4}$$

$$Sensitivity = \frac{TP}{TP + FN}, \tag{5}$$

$$Accuracy = \frac{TP + TN}{TP + TN + FP + FN}, \tag{6}$$

$$MCC = \frac{TP \cdot TN - FP \cdot FN}{\sqrt{(TP + FP) \cdot (TP + FN) \cdot (TN + FP) \cdot (TN + FN)}}, \tag{7}$$

where TP, FP, TN, and FN denote true positive, false positive, true negative, and false negative, respectively. However, the above four evaluation indexes are threshold dependent and it is well known that *Accuracy* is not an appropriate evaluation criterion under the imbalanced learning scenario. In view of this, we also exploited *AUC*, which is the area under the receiver operating characteristic (*ROC*) curve and has been proved to be a reliable performance measure for imbalanced problems [62], as evaluation index. The *AUC* is threshold independent and is often used to evaluate the overall prediction quality of a prediction model.

3.1 Five-Fold Cross-Validation Results on Training Data Sets

In this section, we evaluate the performance of the proposed method by performing fivefold cross-validation on training data sets of the 12 considered ligands separately.

As stated in Section 2.3, protein-ligand binding sites prediction is a typical imbalanced learning problem, where the number of samples in minority class (binding residues) is significantly less that of samples in majority class (nonbinding residues). Under the imbalanced learning scenario, over pursuing the overall accuracy is not appropriate and can be deceiving for evaluating the performance of a predictor. In general, people would expect that a predictor can provide high accuracy of the minority class (e.g., binding residues in this study) without severely jeopardizing the accuracy of the majority class (nonbinding residues) [62]. In view of this, together with the fact that the *MCC* provides the overall measurement of the quality of the binary predictions, we thus reported the threshold-dependent evaluation indexes (e.g., *Sen*, *Spe*, *Acc*, and *MCC*) by choosing the threshold, denoted as T, which maximizes the value of *MCC* of predictions. The performances of the proposed method together with the identified thresholds on the training data sets of the 12 considered ligands over fivefold cross-validation were also listed in Table 4.

Note that since the TargetS is a ligand-specific predictor where the training data sets differ for 12 ligand types, thus the thresholds identified by maximizing *MCC* criteria will also be different accordingly. However, it is interesting for us to find that the thresholds are similar for those ligands belonging to the same category (e.g., ATP, ADP, AMP, GDP, and GTP belonging to Nucleotide category; Ca^{2+}, Mg^{2+}, Mn^{2+}, Fe^{3+}, and Zn^{2+} belonging to Metal Ion category) as shown in Table 4.

By observing Table 4, we can find that the proposed TargetS can generate accurate predictions for all the 12 considered ligands. The *Specificity* (*Spe*) varies from 94.5 to 99.8 percent, the *Accuracy* (*Acc*) from 89.9 to 99.0 percent, the *Matthews correlation coefficient* (*MCC*) from 0.320 to 0.644, and the area under the curve (*AUC*) from 0.784 to 0.938.

We found that for the five types of nucleotide ligands, i.e., ATP, ADP, AMP, GDP, and GTP, the proposed method achieves very similar performances, where *AUC*s varies

TABLE 4
Performance of the Proposed Method on the Training Data Sets of the 12 Types of Ligands over Fivefold Cross Validation

Category	Ligand Type	Threshold *	*Sen* (%)	*Spe* (%)	*Acc* (%)	*MCC*	*AUC*
Nucleotide	ATP	$T_{ATP} = 0.50$	48.4	98.2	96.2	0.492	0.887
	ADP	$T_{ADP} = 0.50$	56.1	98.8	97.2	0.591	0.907
	AMP	$T_{AMP} = 0.50$	38.0	98.2	96.0	0.386	0.856
	GDP	$T_{GDP} = 0.43$	63.9	98.7	97.2	0.644	0.908
	GTP	$T_{GTP} = 0.50$	48.0	98.7	96.9	0.506	0.858
Metal Ion	Ca^{2+}	$T_{Ca} = 0.69$	19.2	99.7	98.4	0.320	0.784
	Mg^{2+}	$T_{Mg} = 0.81$	26.4	99.8	99.0	0.383	0.798
	Mn^{2+}	$T_{Mn} = 0.74$	40.8	99.5	98.7	0.445	0.901
	Fe^{3+}	$T_{Fe} = 0.81$	51.8	99.6	98.8	0.592	0.922
	Zn^{2+}	$T_{Zn} = 0.83$	50.0	99.6	98.9	0.557	0.938
	DNA	$T_{DNA} = 0.49$	41.7	94.5	89.9	0.362	0.824
	HEME	$T_{HEME} = 0.65$	50.5	98.3	94.4	0.579	0.887

* *For each type of ligands, say Mg^{2+}, the threshold T_{Mg} was identified by maximizing the MCC value of predictions on the corresponding training dataset over five-fold cross-validation.*

from 0.856 to 0.908. It is easy to understand this phenomenon as these five types of ligands possess similar sizes, roles, and distributions. According to this justification, we speculate that the proposed method will also achieve similar performances for the five metal ion ligands. However, among the five metal ion ligands, Ca^{2+} and Mg^{2+} perform much worse than other three metal ion ligands. The *AUC*s for Ca^{2+} and Mg^{2+} are less than 0.80, while the *AUC*s for other three metal ions are all greater than 0.90. There exists almost 10 percent gap between them. The potential reasons for this gap will be investigated in the subsequent section.

3.2 Why Ca^{2+} and Mg^{2+} Perform Worse Than Zn^{2+}, Mn^{2+}, and Fe^{3+}?

As stated in Section 2.2, each type of metal ion favors to bind some specific types of residues and the metal ion binding propensity was utilized as indexes to guide the identification process of prediction. Now, we seek to explain why Ca^{2+} and Mg^{2+} perform much worse than Zn^{2+}, Mn^{2+}, and Fe^{3+} from the view of metal ion binding propensity. By revisiting Fig. 1, two observations can be drawn as follows:

1. For all the five types of metal ion ligands, the frequencies of the 20 native amino acids, which are almost the same among nonbinding residues, differ significantly among binding residues.
2. The difference between frequencies of the 20 native amino acids among binding residues and that among nonbinding residues differs significantly for different types of metal ions. We believe that this difference will influence the prediction performance.

For the purpose of quantitative analysis, here we define the *frequency difference index*, denoted as h_{dif}, for metal ion ligand as follows:

$$h_{dif} = \sum_{i=1}^{20} \left| f_b^i - f_{nb}^i \right|, \tag{8}$$

where f_b^i and f_{nb}^i are the frequencies of the ith type of the 20 native amino acids among binging and nonbinding residues, respectively. We calculated that the *frequency difference indexes* for Ca^{2+}, Mg^{2+}, Mn^{2+}, Fe^{3+}, and Zn^{2+} are 73.06, 77.76, 118.09, 129.76, and 154.31, respectively.

We argue that the larger the *frequency difference index*, the better the prediction performance. As the frequency difference indexes for Ca^{2+} and Mg^{2+} are 73.06 and 77.76, respectively, which are the lowest two among the five frequency difference indexes, thus it is foreseeable that the prediction performances for Ca^{2+} and Mg^{2+} will also be the worst as demonstrated in Table 4. To further validate our argument, let's take Mn^{2+}, Fe^{3+}, and Zn^{2+} for consideration: the frequency difference index for Mn^{2+} is 118.09, which are less than that for Fe^{3+} (129.76) and Zn^{2+} (154.31), we thus expect that the prediction performance for Mn^{2+} will be worse than that for Fe^{3+} and Zn^{2+}, and the Zn^{2+} will perform best. From Table 4, we found that the *AUC*s, which are often used to evaluate the overall prediction quality of models, for Mn^{2+}, Fe^{3+}, and Zn^{2+} are 0.901, 0.922, and 0.938, respectively. The results obviously support our speculation.

3.3 Ligand-Specific Model Helps to Improve Prediction Performance

In this section, we will empirically demonstrate that the proposed ligand-specific prediction model is superior to general-purpose prediction model which does not distinguish the types of ligands.

We carried out general-purpose prediction experiments as follows: training data sets of the 12 types of considered ligands were merged to obtain a combined training data set; then, a fivefold cross-validation procedure was performed on the combined training data set. Note that in each round of cross-validation, the positive samples were those binding residues regardless of the types of ligands they bind to, while the negative samples were those nonbinding residues accordingly. In the evaluation stage, performances were calculated for each type of ligands individually. Note that

as we do not distinguish the ligand types in this experiment, thus the binding propensity feature were obtained based on the frequencies of the 20 native amino acids among binding residues regardless of the types of ligands they bind to.

The performance comparisons between the general-purpose and ligand-specific predictions on the training data sets of the 12 considered ligands are listed in Table S1, which can be found in the online supplemental material available on the Computer Society Digital Library at http://doi.ieeecomputersociety.org/10.1109/TCBB.2013.104. Note that for the convenience of comparison, we restricted the false positive rate (FPR) of predictions to be (or most close to) 5 percent.

By observing Table S1, which is available in the online supplemental material, it is easy to find that the other four evaluation indexes, i.e., *Sen*, *Acc*, *MCC*, and *AUC*, of ligand-specific predictions are consistently superior to that of general-purpose predictions under the same *Spe* (95 percent or most close to 95 percent) for all the 12 considered ligands. Particularly, ligand-specific predictions significantly outperform general-purpose predictions on the *Sen* and *MCC* and averaged improvements of 14.6 and 10.0 percent were achieved, respectively. As to *AUC*, the index for evaluating the overall prediction quality of predictions, the ligand-specific method also outperforms general-purpose method with an averaged improvement of 4.7 percent.

Experimental results listed in Table S1, which is available in the online supplemental material, demonstrate that the ligand-specific method is superior to general-purpose method, at least on the tested benchmark data sets. These improvements may result from the following two aspects: On the one hand, ligand-specific method performs predictions for different ligands with corresponding specialized prediction models, which can accommodate the differences of roles, sizes, and distributions existed in different types of ligands much better. On the other hand, in general-purpose method, binding propensity feature is calculated based on the frequencies of the 20 native amino acids among binding residues regardless of the types of ligands they bind to, while in ligand-specific method, binding propensity feature is calculated for each type of ligands respectively thus can characterize the ligand binding propensities of residues much well. We believe this ligand-specific binding propensity feature possess much better discrimination capability, which maybe one of the most important factors that account for the performance improvements.

3.4 Comparison with Existing Predictors

In this section, we will experimentally demonstrate the efficacy of the proposed TargetS by comparing it with other popular predictors via independent test and blind test as follows:

3.4.1 Independent Test on Validation Data Sets

For each type of ligands, we compared TargetS with two other ligand-specific predictors and one alignment-based baseline predictor on the independent validation data set.

Ligand-specific predictors for comparison differ for different types of ligands. More specifically, NsitePred [30], a most recently developed predictor specifically designed for predicting nucleotide-binding residues, and SVMPred [7] were chosen for comparison for the five types of nucleotide ligands; FunFOLD [73] and CHED [74] were taken as ligand-specific predictors for comparison for the five types of metal ion ligands; Note that FunFOLD was initially designed for general-purpose binding sites prediction. In this study, we retrained the FunFOLD on the data set of each type of the five metal ion ligands and used it as ligand-specific predictor. MetaDBSite [75], a meta approach for protein-DNA binding sites prediction, and DNABR [76] were used as ligand-specific predictors for comparison for the DNA ligand; finally, HemeNet [37] and HemeBind [12], which are the only two available predictors (to the best of our knowledge) that were specifically designed for predicting HEME binding residues. As the webserver of HemeNet doest not work currently, thus only HemeBind was taken for comparison for HEME ligand. Note that when performing comparisons between TargetS and the above-mentioned ligand-specific predictors, we trained our TargetS using training data set for that ligand and tested it with the corresponding independent validation data set (see Table 1), while prediction results of other ligand-specific predictors were obtained by feeding sequences or 3D structures in the independent validation data set to their corresponding web servers. As SVMPred does not provide a web server, we thus locally implemented it based on our training data sets of the five nucleotide ligands and tested it with the corresponding independent validation data sets.

Alignment-based predictions were performed as follows: for each query sequence in a validation data set, we executed the alignment-based prediction by aligning the query sequence and all the sequences in the corresponding training data set. The residues in the query sequence that were aligned with the binding residues of the best aligned sequence are predicted as the binding residues.

Table 5 illustrates the performance comparison of TargetS with NsitePred, SVMPred, and alignment-based predictor on the independent validation data sets of the five nucleotide ligands. Considering the page limit, comparison results for other seven types of ligands, i.e., Ca^{2+}, Mg^{2+}, Mn^{2+}, Fe^{3+}, Zn^{2+}, DNA, and HEME are listed in the supplemental materials (see Tables S2, S3, and S4, which are available in the online supplemental material).

From Table 5, we can find that the *AUC*s for ATP, ADP, AMP, GDP, and GTP on the corresponding independent validation data sets are 0.898, 0.896, 0.830, 0.896, and 0.855, respectively. By revisiting Table 4, it is found that the *AUC*s for ATP, ADP, AMP, GDP, and GTP on the training data sets are 0.887, 0.907, 0.856, 0.908, and 0.858, respectively. In other words, for all the five nucleotide ligands, TargetS achieves similar overall prediction performances (measured by *AUC*s) on the training data set and independent validation data set, denoting that the generalization capability of the TargetS derived from the knowledge buried in training data sets has not been over- or underestimated.

By observing Table 5, it is found that the alignment-based predictor achieve very similar performances on *Spe* ($\geq 97\%$) to other three machine-learning-based predictors. However, its performances on *Sen* are poorest (i.e., the alignment-based predictor predicts too many false

TABLE 5
Performance Comparison of TargetS with NsitePred, SVMPred, and Alignment-Based Predictor on the Independent Validation Data Sets of the Five Nucleotide Ligands

Ligand Type	Predictor	*Sen* (%)	*Spe* (%)	*Acc* (%)	*MCC*	*AUC*
ATP	TargetS	50.1	**98.3**	**96.5**	**0.502**	0.898
	NsitePred	**50.8**	97.3	95.5	0.439	-
	SVMPred	47.3	96.7	94.9	0.387	0.877
	alignment-based	30.6	97.0	94.5	0.265	-
ADP	TargetS	**46.9**	**98.9**	**97.2**	**0.507**	0.896
	NsitePred	46.2	97.6	96.0	0.419	-
	SVMPred	46.1	97.2	95.5	0.382	0.875
	alignment-based	31.8	97.4	95.1	0.284	-
AMP	TargetS	**34.2**	**98.2**	**95.9**	**0.359**	0.830
	NsitePred	33.9	97.6	95.3	0.321	-
	SVMPred	32.1	96.4	94.1	0.255	0.798
	alignment-based	19.6	97.3	94.5	0.178	-
GDP	TargetS	**56.2**	**98.1**	**96.2**	**0.550**	0.896
	NsitePred	55.7	97.9	96.1	0.536	-
	SVMPred	49.5	97.6	95.4	0.466	0.870
	alignment-based	41.2	97.8	95.3	0.415	
GTP	TargetS	57.3	**98.8**	**96.9**	**0.617**	0.855
	NsitePred	**58.4**	95.7	94.0	0.448	-
	SVMPred	48.3	91.7	89.7	0.276	0.821
	alignment-based	52.8	97.9	95.9	0.516	-

negatives) resulting in low *MCC*s for all the five types of nucleotide ligands only except for GTP.

We also find that that the three machine-learning-based predictors almost always perform better than the alignment-based predictor. Among the three machine-learning-based predictors, the proposed TargetS consistently performs the best on *Spe*, *Acc*, and *MCC* for all the five nucleotide ligands and acts as the best performance. Compared with the second-best performer, i.e., NsitePred, TargetS achieves averaged improvements of 1.2, 1.1, and 7.3 percent on *Spe*, *Acc*, and *MCC*, respectively, while still possesses almost the equal performance on *Sen* as NsitePred at the same time.

3.4.2 Blind Test on CASP9 Data Set

As described in Section 2.1, 30 protein sequences in CASP9 data set were used for blind test. Considering that the sequences in CASP9 interact with many different types of ligands, we thus compare TargetS with several popular general-purpose rather than ligand-specific predictors. ConSeq [77], a webserver for the identification of biologically important residues in protein sequences, was chosen as the sequence-based general-purpose predictor for comparison, while SITEHOUND [19] and MetaPocket [78] were chosen as the structure-based general-purpose predictors for comparison.

The prediction results of ConSeq [77], SITEHOUND [19], and MetaPocket [78] were obtained by feeding 30 protein sequences or 3D structures to their corresponding webservers, while the prediction results of TargetS were obtained as follows: For each blind test protein sequence, we fed it to the 12 ligand-specific prediction models, respectively, and the predicted binding residues of the 12 models were then merged as the final prediction results for that sequence. Table 6 compares the performance of TargetS with ConSeq [77], SITEHOUND [19], and MetaPocket [78] for the 30 targets in CASP9.

According to the *MCC*, which is the overall measurement of the quality of the binary predictions, listed in Table 6, we can find that the TargetS acts as the best performer followed by MetaPocket, SITEHOUND, and ConSeq. TargetS significantly outperforms the other sequence-based predictor, i.e., ConSeq [77], on all the four evaluation indexes and an improvement of 20 percent on *MCC* was achieved. In addition, TargetS also overwhelms the structure-based predictor SITEHOUND. The *Sen*, *Acc*, and *MCC* of TargetS are 38.9, 94.2, and 0.317 percent, respectively, which are 16.4,

TABLE 6
Performance Comparison of TargetS with ConSeq, SITEHOUND and MetaPocket for the 30 Targets in CASP9

Predictor	*Sen* (%)	*Spe* (%)	*Acc* (%)	*MCC*
TargetS	38.9	**96.5**	**94.2**	**0.317**
MetaPocket [78]	**70.4**	80.0	79.7	0.237
SITEHOUND [19]	22.5	95.1	92.3	0.149
ConSeq [77]	32.1	87.7	85.5	0.114

1.9, and 16.8 percent higher than that of SITHOUND, which is the third-best performer. We also found that the second-best performer, i.e., MetaPocket, achieves the highest *Sen* (70.4 percent), which is almost twice that, i.e., 38.9 percent, of the TargetS. However, the *Spe* of MetaPocket is only 80.0 percent which is lowest one among the four considered predictors. In other words, MetaPocket predicts too many false positives (nonbinding residues are predicted as binding ones), thus the reliability of the predicted binding residues of MetaPocket is the lowest among the listed predictors.

Currently, TargetS embraces 12 types of ligands and most types of ligands contained in CASP9 were in fact not covered by TargetS. However, by observing Table 6, we can find that TargetS still achieves satisfactory performances for the 30 blind test proteins and acts as the best performer among the four listed predictors. We speculate that is due to the multiple ligands coverage of TargetS and the hypothesis that binding residues for different ligands can share some common features, TargetS can thus yield good prediction results for the ligands that not belonging to the 12 types.

3.4.3 Performing Comparison on Benchmark Data Set That Has Been Used by Other Predictors

Except for the independent validation test and blind test performed above, we will try to further demonstrate the efficacy of the proposed TargetS by comparing it with other predictors based on the same benchmark data set that has been used by the compared predictors. Taking protein-nucleotide binding sites prediction as an example, the data set 1 constructed by Chen et al. [30] was taken as the benchmark data set. The data set 1 [30] consists of 227, 321, 140, 56, and 105 sequences that bind to ATP, ADP, AMP, GTP, and GDP, respectively, and the maximal pairwise sequence identity of the sequences among each type of the five nucleotides was less than 40 percent.

We compared TargetS with SVMPred [7], Rate4site [23], and NsitePred [30] on data set 1 over fivefold cross-validation as done in [30] and the comparison results were listed in Table 7. By observing Table 7, we found that the TargetS obtains $AUC > 0.85$, $MCC > 0.41$ for all the five types of nucleotide ligands. The *AUC* and *MCC* values of TargetS are consistently superior to that of all the other three considered predictors, i.e., SVMPred [7], Rate4site [23], and NsitePred [30] and the averaged improvements of 2.3 and 5.4 percent were achieved, respectively, if compared with the second-best performer NsitePred [30]. It has not escaped from our notice that Rate4site [23] achieves highest *Sen* values, i.e., 56.2 and 56.9 percent for AMP and GTP, respectively. However, the corresponding *Spe* values are much lower, i.e., 79.9 and 80.6 percent, denoting too many false positives were incurred during prediction. On the other hand, SVMPred [7] achieves the best performances on *Spe* for several nucleotide ligands (i.e., 99.3, 99.6, and 99.7 percent for ADP, AMP, and GTP, respectively) while with much lower *Sen* values implying too many false negatives were produced during prediction.

TABLE 7
Performance Comparison of the Proposed TargetS with Other Protein-Nucleotide Binding Sites Predictors on the Benchmark Data Set 1 in [30] over Fivefold Cross Validation

Ligand Type	Predictor	*Sen* (%)	*Spe* (%)	*Acc* (%)	*MCC*	*AUC*
ATP	**TargetS**	**44.6**	**99.0**	**96.7**	**0.531**	**0.896**
	NsitePred *	44.4	98.2	96.0	0.460	0.861
	SVMPred *	36.1	98.8	96.2	0.433	0.854
	Rate4site *	44.6	87.0	85.2	0.182	0.749
ADP	**TargetS**	**58.7**	99.0	**97.5**	**0.631**	**0.918**
	NsitePred *	54.4	98.8	97.1	0.572	0.893
	SVMPred *	45.8	**99.3**	97.3	0.555	0.885
	Rate4site *	47.2	84.4	83.0	0.161	0.749
AMP	**TargetS**	36.8	98.6	96.1	**0.418**	**0.857**
	NsitePred *	30.4	98.8	96.2	0.377	0.829
	SVMPred *	20.8	**99.6**	**96.6**	0.360	0.820
	Rate4site *	**56.2**	79.9	79.0	0.174	0.755
GDP	**TargetS**	**65.0**	**99.6**	**98.1**	**0.741**	**0.920**
	NsitePred *	64.6	99.1	97.6	0.675	0.910
	SVMPred *	62.3	98.9	97.7	0.655	0.905
	Rate4site *	51.6	82.3	81.1	0.170	0.733
GTP	**TargetS**	44.3	99.6	**97.4**	**0.595**	**0.863**
	NsitePred *	47.3	99.1	96.8	0.562	0.844
	SVMPred *	37.3	**99.7**	97.0	0.551	0.836
	Rate4site *	**56.9**	80.6	79.6	0.180	0.748

* *Data excerpted from [30].*

4 Conclusions

We have designed and implemented a ligand-specific template-free predictor, called TargetS, for predicting protein-ligand binding sites. TargetS was trained on data collected from a most recently released protein-ligand interaction database BioLip [45] with our proposed *modified AdaBoost* (*MAdaBoost*) learning algorithm [79]. Experimental results on training data sets, independent validation data sets and blind test on CASP9 data set have demonstrated the efficacy of the proposed TargetS. The success of TargetS is due to several reasons include good benchmark data sets, ligand-specific propensity discriminative feature design, careful construction of the prediction model and the spatial clustering algorithm. Currently, the TargetS prediction server has already been put online and been able to predict binding sites for 12 types of ligands. Our future woks will focus on further incorporating binding sites prediction modules for other new types of ligands into TargetS to enhance its capability. In addition, we will also continue to improve the prediction accuracy of TargetS by developing new effective feature extraction methods and applying more powerful classifiers.

In the current work, a major problem of TargetS is that the computation time is relatively long (about 325 s for a sequence with 300 residues), although it is fast than many template-based methods such as MetaPocket, because the TargetS have to perform PSI-BLAST [57], PSIPRED [59], and MODELLER [43] to extract features and model the 3D structure from a protein sequence. We will also try to accelerate the computation speed by using several servers to parallely perform these computations in the future.

Acknowledgments

The authors would like to thank the anonymous reviewers for suggestions and comments which helped improve the quality of this paper. This work was supported by the National Natural Science Foundation of China (no. 61373062, 91130033, 61175024, 61222306, and 61233011), the Jiangsu Postdoctoral Science Foundation

(no. 1201027C), the China Postdoctoral Science Foundation (no. 2013M530260), the Fundamental Research Funds for the Central Universities, (no. 30920130111010), the Foundation for the Author of National Excellent Doctoral Dissertation of PR China (no. 201048), and the Shanghai Science and Technology Commission (no. 11JC1404800). H.B. Shen is the corresponding author for this paper.

REFERENCES

[1] B. Alberts, *Molecular Biology of the Cell,* fifth ed. Garland Science, 2008.

[2] M. Gao and J. Skolnick, "The Distribution of Ligand-Binding Pockets Around Protein-Protein Interfaces Suggests a General Mechanism for Pocket Formation," *Proc. Nat'l Academy of Science USA,* vol. 109, no. 10, pp. 3784-3789, Mar. 2012.

[3] H. Kokubo, T. Tanaka, and Y. Okamoto, "Ab Initio Prediction of Protein-Ligand Binding Structures by Replica-Exchange Umbrella Sampling Simulations," *J. Computational Chemistry,* vol. 32, no. 13, pp. 2810-2821, Oct. 2011.

[4] P. Schmidtke and X. Barril, "Understanding and Predicting Druggability. A High-Throughput Method for Detection of Drug Binding Sites," *J. Medicinal Chemistry,* vol. 53, no. 15, pp. 5858-5867, Aug. 2010.

[5] H.M. Berman et al., "The Protein Data Bank," *Nucleic Acids Research,* vol. 28, no. 1, pp. 235-242, 2000.

[6] J.S. Chauhan, N.K. Mishra, and G.P. Raghava, "Identification of ATP Binding Residues of a Protein from Its Primary Sequence," *BMC Bioinformatics,* vol. 10, article 434, 2009.

[7] K. Chen, M.J. Mizianty, and L. Kurgan, "ATPsite: Sequence-Based Prediction of ATP-Binding Residues," *Proteome Science,* vol. 9, no. Suppl 1, article S4, 2011.

[8] S. Leis, S. Schneider, and M. Zacharias, "In Silico Prediction of Binding Sites on Proteins," *Current Medicinal Chemistry,* vol. 17, no. 15, pp. 1550-1562, 2010.

[9] A. Roy and Y. Zhang, "Recognizing Protein-Ligand Binding Sites by Global Structural Alignment and Local Geometry Refinement," *Structure,* vol. 20, no. 6, pp. 987-997, June 2012.

[10] M. Brylinski and J. Skolnick, "FINDSITE: A Threading-Based Approach to Ligand Homology Modeling," *PLoS Computational Biology,* vol. 5, no. 6, article e1000405, June 2009.

[11] A.T. Laurie and R.M. Jackson, "Methods for the Prediction of Protein-Ligand Binding Sites for Structure-Based Drug Design and Virtual Ligand Screening," *Current Protein and Peptide Science,* vol. 7, no. 5, pp. 395-406, Oct. 2006.

[12] R. Liu and J. Hu, "HemeBIND: A Novel Method for Heme Binding Residue Prediction by Combining Structural and Sequence Information," *BMC Bioinformatics,* vol. 12, article 207, 2011.

[13] M. Hendlich, F. Rippmann, and G. Barnickel, "LIGSITE: Automatic and Efficient Detection of Potential Small Molecule-Binding Sites in Proteins," *J. Molecular Graphics and Modelling,* vol. 15, no. 6, pp. 359-363, Dec. 1997.

[14] J. Dundas et al., "CASTp: Computed Atlas of Surface Topography of Proteins with Structural and Topographical Mapping of Functionally Annotated Residues," *Nucleic Acids Research,* vol. 34, no. Web Server issue, pp. W116-W118, July 2006.

[15] R.A. Laskowski, "SURFNET: A Program for Visualizing Molecular Surfaces, Cavities, and Intermolecular Interactions," *J. Molecular Graphics,* vol. 13, no. 5, pp. 323-330, Oct. 1995.

[16] D.G. Levitt and L.J. Banaszak, "POCKET: A Computer Graphics Method for Identifying and Displaying Protein Cavities and Their Surrounding Amino Acids," *J. Molecular Graphics,* vol. 10, no. 4, pp. 229-34, Dec. 1992.

[17] V. Le Guilloux, P. Schmidtke, and P. Tuffery, "Fpocket: an Open Source Platform for Ligand Pocket Detection," *BMC Bioinformatics,* vol. 10, article 168, 2009.

[18] A.T. Laurie and R.M. Jackson, "Q-SiteFinder: An Energy-Based Method for the Prediction of Protein-Ligand Binding Sites," *Bioinformatics,* vol. 21, no. 9, pp. 1908-1916, May 2005.

[19] M. Hernandez, D. Ghersi, and R. Sanchez, "SITEHOUND-Web: A Server for Ligand Binding Site Identification in Protein Structures," *Nucleic Acids Research,* vol. 37, no. Web Server issue, pp. W413-W416, July 2009.

[20] B. Hoffmann et al., "A New Protein Binding Pocket Similarity Measure Based on Comparison of Clouds of Atoms in 3D: Application to Ligand Prediction," *BMC Bioinformatics,* vol. 11, article 99, 2010.

[21] A. Kahraman et al., "Shape Variation in Protein Binding Pockets and Their Ligands," *J. Molecular Biology,* vol. 368, no. 1, pp. 283-301, Apr. 2007.

[22] A. Armon, D. Graur, and N. Ben-Tal, "ConSurf: An Algorithmic Tool for the Identification of Functional Regions in Proteins by Surface Mapping of Phylogenetic Information," *J. Molecular Biology,* vol. 307, no. 1, pp. 447-463, Mar. 2001.

[23] T. Pupko et al., "Rate4Site: An Algorithmic Tool for the Identification of Functional Regions in Proteins by Surface Mapping of Evolutionary Determinants within Their Homologues," *Bioinformatics,* vol. 18, no. Suppl 1, pp. S71-S77, 2002.

[24] Y. Dou et al., "L1pred: A Sequence-Based Prediction Tool for Catalytic Residues in Enzymes with the L1-Logreg Classifier," *PLoS One,* vol. 7, no. 4, article e35666, 2012.

[25] B. Huang and M. Schroeder, "LIGSITEcsc: Predicting Ligand Binding Sites Using the Connolly Surface and Degree of Conservation," *BMC Structural Biology,* vol. 6, article 19, 2006.

[26] J.A. Capra et al., "Predicting Protein Ligand Binding Sites by Combining Evolutionary Sequence Conservation and 3D Structure," *PLoS Computational Biology,* vol. 5, no. 12, article e1000585, Dec. 2009.

[27] F. Glaser et al., "A method for Localizing Ligand Binding Pockets in Protein Structures," *Proteins,* vol. 62, no. 2, pp. 479-488, Feb. 2006.

[28] P. Aloy et al., "Structure-Based Assembly of Protein Complexes in Yeast," *Science,* vol. 303, no. 5666, pp. 2026-2029, Mar. 2004.

[29] L. Lu et al., "Multimeric Threading-Based Prediction of Protein-Protein Interactions on a Genomic Scale: Application to the *Saccharomyces cerevisiae* Proteome," *Genome Research,* vol. 13, no. 6A, pp. 1146-1154, June 2003.

[30] K. Chen, M.J. Mizianty, and L. Kurgan, "Prediction and Analysis of Nucleotide-Binding Residues Using Sequence and Sequence-Derived Structural Descriptors," *Bioinformatics,* vol. 28, no. 3, pp. 331-341, Feb. 2012.

[31] F. Ferre and P. Clote, "DiANNA 1.1: An Extension of the DiANNA Web Server for Ternary Cysteine Classification," *Nucleic Acids Research,* vol. 34, no. Web Server issue, pp. W182-W185, July 2006.

[32] A. Passerini et al., "Identifying Cysteines and Histidines in Transition-Metal-Binding Sites Using Support Vector Machines and Neural Networks," *Proteins,* vol. 65, no. 2, pp. 305-316, Nov. 2006.

[33] A. Passerini, M. Lippi, and P. Frasconi, "Predicting Metal-Binding Sites from Protein Sequence," *IEEE/ACM Trans. Computational Biology and Bioinformatics,* vol. 9, no. 1, pp. 203-213, Jan./Feb. 2012.

[34] S. Henrich et al., "Computational Approaches to Identifying and Characterizing Protein Binding Sites for Ligand Design," *J. Molecular Recognition,* vol. 23, no. 2, pp. 209-219, Mar./Apr. 2010.

[35] M.M. Gromiha, "Development of RNA Stiffness Parameters and Analysis on Protein-RNA Binding Specificity: Comparison with DNA," *Current Bioinformatics,* vol. 7, no. 2, pp. 173-179, June 2012.

[36] M.M. Gromiha et al., "Sequence and Structural Features of Binding Site Residues in Protein-Protein Complexes: Comparison with Protein-Nucleic Acid Complexes," *Proteome Science,* vol. 9, no. Suppl 1, article S13, 2011.

[37] R. Liu and J. Hu, "Computational Prediction of Heme-Binding Residues by Exploiting Residue Interaction Network," *PLoS One,* vol. 6, no. 10, article e25560, 2011.

[38] J.S. Sodhi et al., "Predicting Metal-Binding Site Residues in Low-Resolution Structural Models," *J. Molecular Biology,* vol. 342, no. 1, pp. 307-320, Sept. 2004.

[39] M. Brylinski and J. Skolnick, "FINDSITE-Metal: Integrating Evolutionary Information and Machine Learning for Structure-Based Metal-Binding Site Prediction at the Proteome Level," *Proteins,* vol. 79, no. 3, pp. 735-751, Mar. 2011.

[40] M. Kumar, A.M. Gromiha, and G.P.S. Raghava, "Prediction of RNA Binding Sites in a Protein Using SVM and PSSM Profile," *Proteins-Structure Function and Bioinformatics,* vol. 71, no. 1, pp. 189-194, Apr. 2008.

[41] V.N. Vapnik, *Statistical Learning Theory.* Wiley-Interscience, 1998.

[42] R.E. Fan, P.H. Chen, and C.J. Lin, "Working Set Selection Using Second Order Information for Training SVM," *J. Machine Learning Research,* vol. 6, pp. 1889-1918, 2005.

[43] M.A. Marti-Renom et al., "Comparative Protein Structure Modeling of Genes and Genomes," *Ann. Rev. Biophysics and Biomolecular Structure,* vol. 29, pp. 291-325, 2000.

[44] P.W. Rose et al., "The RCSB Protein Data Bank: Redesigned Web Site and Web Services," *Nucleic Acids Research,* vol. 39, no. Database issue, pp. D392-D401, Jan. 2011.

[45] J. Yang, A. Roy, and Y. Zhang, "BioLiP: A Semi-Manually Curated Database for Biologically Relevant Ligand-Protein Interactions," *Nucleic Acids Research,* vol. 41, no. D1, pp. D1096-D1103, Jan. 2013.

[46] B.H. Dessailly et al., "LigASite-A Database of Biologically Relevant Binding Sites in Proteins with Known Apo-Structures," *Nucleic Acids Research,* vol. 36, no. Database issue, pp. D667-D673, Jan. 2008.

[47] G. Lopez, A. Valencia, and M. Tress, "FireDB—A Database of Functionally Important Residues from Proteins of Known Structure," *Nucleic Acids Research,* vol. 35, no. Database issue, pp. D219-D223, Jan. 2007.

[48] R. Wang et al., "The PDBbind Database: Collection of Binding Affinities for Protein-Ligand Complexes with Known Three-Dimensional Structures," *J. Medicinal Chemistry,* vol. 47, no. 12, pp. 2977-2980, June 2004.

[49] G. Wang and R.L. Dunbrack Jr., "PISCES: A Protein Sequence Culling Server," *Bioinformatics,* vol. 19, no. 12, pp. 1589-1591, Aug. 2003.

[50] J.C. Jeong, X. Lin, and X.W. Chen, "On Position-Specific Scoring Matrix for Protein Function Prediction," *IEEE/ACM Trans. Computational Biology and Bioinformatics,* vol. 8, no. 2, pp. 308-315, Mar./Apr. 2011.

[51] Y.N. Zhang et al., "Predicting Protein-ATP Binding Sites from Primary Sequence through Fusing Bi-Profile Sampling of Multi-View Features," *BMC Bioinformatics,* vol. 13, article 118, 2012.

[52] D.J. Yu, H.B. Shen, and J.Y. Yang, "SOMPNN: An Efficient Non-Parametric Model for Predicting Transmembrane Helices," *Amino Acids,* vol. 42, no. 6, pp. 2195-2205, June 2012.

[53] M.H. Zangooei and S. Jalili, "Protein Secondary Structure Prediction Using DWKF Based on SVR-NSGAII," *Neurocomputing,* vol. 94, pp. 87-101, May 2012.

[54] A. Pierleoni, P.L. Martelli, and R. Casadio, "MemLoci: Predicting Subcellular Localization of Membrane Proteins in Eukaryotes," *Bioinformatics,* vol. 27, no. 9, pp. 1224-1230, May 2011.

[55] H.B. Shen and K.C. Chou, "A Top-Down Approach to Enhance the Power of Predicting Human Protein Subcellular Localization: Hum-mPLoc 2.0," *Analytical Biochemistry,* vol. 394, no. 2, pp. 269-274, Nov. 2009.

[56] M.W. Mak, J. Guo, and S.Y. Kung, "PairProSVM: Protein Subcellular Localization Based on Local Pairwise Profile Alignment and SVM," *IEEE/ACM Trans. Computational Biology and Bioinformatics,* vol. 5, no. 3, pp. 416-422, July-Sept. 2008.

[57] A.A. Schaffer, "Improving the Accuracy of PSI-BLAST Protein Database Searches with Composition-Based Statistics and Other Refinements," *Nucleic Acids Research,* vol. 29, pp. 2994-3005, 2001.

[58] K. Chen, M.J. Mizianty, and L. Kurgan, "ATPsite: Sequence-Based Prediction of ATP-Binding Residues," *Proteome Science,* vol. 9, no. Suppl 1, p. S4, 2011.

[59] D.T. Jones, "Protein Secondary Structure Prediction Based on Position-Specific Scoring Matrices," *J. Molecular Biology,* vol. 292, no. 2, pp. 195-202, Sept. 1999.

[60] M.M. Gromiha and K. Fukui, "Scoring Function Based Approach for Locating Binding Sites and Understanding Recognition Mechanism of Protein-DNA Complexes," *J. Chemical Information and Modeling,* vol. 51, no. 3, pp. 721-729, Mar. 2011.

[61] C.H. Lu et al., "Prediction of Metal Ion-Binding Sites in Proteins Using the Fragment Transformation Method," *PLoS One,* vol. 7, no. 6, article e39252, 2012.

[62] H. He and E.A. Garcia, "Learning from Imbalanced Data," *IEEE Trans. Knowledge and Data Eng.,* vol. 21, no. 9, pp. 1263-1284, Sept. 2009.

[63] Z.Y. Lin et al., "Several SVM Ensemble Methods Integrated with Under-Sampling for Imbalanced Data Learning," *Proc. Fifth Int'l Conf. Advanced Data Mining and Applications (ADMA '09),* pp. 536-554, 2009.

[64] P.L. Martelli, P. Fariselli, and R. Casadio, "An ENSEMBLE Machine Learning Approach for the Prediction of All-Alpha Membrane Proteins," *Bioinformatics,* vol. 19, no. Suppl 1, pp. i205-i211, 2003.

[65] L. Nanni, "A Novel Ensemble of Classifiers for Protein Fold Recognition," *Neurocomputing,* vol. 69, nos. 16-18, pp. 2434-2437, Oct. 2006.

[66] L. Nanni, "Ensemble of Classifiers for Protein Fold Recognition," *Neurocomputing,* vol. 69, nos. 7-9, pp. 850-853, Mar. 2006.

[67] J. Wu et al., "An Ensemble Classifier of Support Vector Machines Used to Predict Protein Structural Classes by Fusing Auto Covariance and Pseudo-Amino Acid Composition," *Protein J.,* vol. 29, no. 1, pp. 62-67, Jan. 2010.

[68] G. Rogova, "Combining the Results of Several Neural Network Classifiers," *Neural Networks,* vol. 7, pp. 777-781, 1994.

[69] Y. Freund and R.E. Schapire, "A Decision-Theoretic Generalization of On-Line Learning and an Application to Boosting," *J. Computer and System Sciences,* vol. 55, no. 1, pp. 119-139, 1997.

[70] L.I. Kuncheva, *Combining Pattern Classifiers: Methods and Algorithms.* John Wiley & Sons, 2004.

[71] O. Schueler-Furman and D. Baker, "Conserved Residue Clustering and Protein Structure Prediction," *Proteins,* vol. 52, no. 2, pp. 225-235, Aug. 2003.

[72] D.J. Yu et al., "TargetATPsite: A Template-Free Method for ATP-Binding Sites Prediction with Residue Evolution Image Sparse Representation and Classifier Ensemble," *J. Computational Chemistry,* vol. 34, pp. 974-985, Jan. 2013.

[73] D.B. Roche, S.J. Tetchner, and L.J. McGuffin, "FunFOLD: An Improved Automated Method for the Prediction of Ligand Binding Residues Using 3D Models of Proteins," *BMC Bioinformatics,* vol. 12, article 160, 2011.

[74] M. Babor et al., "Prediction of Transition Metal-Binding Sites from Apo Protein Structures," *Proteins,* vol. 70, no. 1, pp. 208-217, Jan. 2008.

[75] J. Si et al., "MetaDBSite: A Meta Approach to Improve Protein DNA-Binding Sites Prediction," *BMC Systems Biology,* vol. 5, no. Suppl 1, article S7, 2011.

[76] X. Ma et al., "Sequence-Based Prediction of DNA-Binding Residues in Proteins with Conservation and Correlation Information," *IEEE/ACM Trans. Computational Biology and Bioinformatics,* vol. 9, no. 6, pp. 1766-1775, Nov./Dec. 2012.

[77] C. Berezin et al., "ConSeq: The Identification of Functionally and Structurally Important Residues in Protein Sequences," *Bioinformatics,* vol. 20, no. 8, pp. 1322-1324, May 2004.

[78] B.D. Huang, "MetaPocket: A Meta Approach to Improve Protein Ligand Binding Site Prediction," *OMICS,* vol. 13, no. 4, pp. 325-330, Aug. 2009.

[79] D.J. Yu et al., "Improving Protein-ATP Binding Residues Prediction by Boosting SVMs with Random Under-Sampling," *Neurocomputing,* vol. 104, pp. 180-190, 2013.

Dong-Jun Yu received the BS degree in computer science and the MS degree in artificial intelligence from Jiangsu University of Science and Technology, in 1997 and 2000, respectively, and the PhD degree in pattern analysis and machine intelligence from Nanjing University of Science and Technology in 2003. In 2008, he acted as an academic visitor at the University of York in the United Kingdom. He is currently an associate professor at the School of Computer Science and Engineering, Nanjing University of Science and Technology. His current interests include bioinformatics, pattern recognition, and data mining. He is a member of the IEEE and the CCF.

Jun Hu received the BS degree in computer science from Anhui Normal University, China, in 2011. Currently, he is working toward the PhD. degree at the School of Computer Science and Engineering, Nanjing University of Science and Technology, China. His research interests include bioinformatics, data mining, and pattern recognition.

Jing Yang received the BS degree in automation from the North University of China, in 2010. He is working toward the MS degree in pattern recognition at Shanghai Jiao Tong University, China. His research interests include pattern recognition, machine learning algorithms, and bioinformatics.

Hong-Bin Shen received the PhD degree from Shanghai Jiaotong University, China, in 2007. He was a postdoctoral research fellow of Harvard Medical School from 2007 to 2008. Currently, he is a professor at the Institute of Image Processing and Pattern Recognition, Shanghai Jiaotong University. His research interests include data mining, pattern recognition, and bioinformatics. He has published more than 60 papers and constructed 20 bioinformatics severs in these areas, and he serves as editorial board member of several international journals.

Jinhui Tang received the BE and PhD degrees both from the University of Science and Technology of China, in 2003 and 2008, respectively. He is currently a professor at the School of Computer Science and Engineering, Nanjing University of Science and Technology. His current research interests include large-scale multimedia search, social media mining, and computer vision. He has authored more than 80 journal and conference papers in these areas. He serves as an editorial board member of *Pattern Analysis and Applications, Multimedia Tools and Applications, Information Sciences, Neurocomputing*; a technical committee member for about 30 international conferences; and a reviewer for about 30 prestigious international journals. He is a corecipient of the Best Paper Award from ACM Multimedia 2007, PCM 2011, and ICIMCS 2011. He is a member of the IEEE, the ACM, and the CCF.

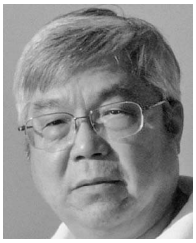

Jing-Yu Yang received the BS degree in computer science from Nanjing University of Science and Technology (NUST), China. From 1982 to 1984, he was a visiting scientist at the Coordinated Science Laboratory, University of Illinois at Urbana-Champaign. From 1993 to 1994, he was a visiting professor in the Department of Computer Science, Missouri University, and in 1998, he acted as a visiting professor at Concordia University, Canada. He is currently a professor and chairman in the Department of Computer Science at NUST. His current research interests include the areas of pattern recognition, robot vision, image processing, data fusion, and artificial intelligence. He is the author of more than 150 scientific papers on computer vision, pattern recognition, and artificial intelligence. He has won more than 20 provincial awards and national awards.